INSTITUTE OF PHYSICS PUBLISHING JOURNAL OF PHYSICS D: APPLIED PHYSICS

J. Phys. D: Appl. Phys. **36** (2003) 1689–1695 PII: S0022-3727(03)57024-3

Imaging fluorescence lifetime modulation of a ruthenium-based dye in living cells: the potential for oxygen sensing

Wei Zhong, Paul Urayama and Mary-Ann Mycek[1]

Department of Biomedical Engineering, 2111 Carl A. Gerstacker Building, 2200 Bonisteel Boulevard, University of Michigan, Ann Arbor, MI 48109-2099, USA

E-mail: mycek@umich.edu

Received 3 December 2002, in final form 27 March 2003
Published 1 July 2003
Online at stacks.iop.org/JPhysD/36/1689

Abstract

Fluorescence lifetime measurements of long excited-state lifetime, oxygen-quenched ruthenium dyes are emerging as methods for intracellular oxygen sensing. Fluorescence lifetime imaging microscopy (FLIM) studies in cells have been reported previously. Many current FLIM systems use high repetition rate ($\sim 10^7$ Hz) lasers optimized for nanosecond lifetime measurements, making measurement of long, microsecond lifetime fluorophores difficult. Here, we present an experimental approach for obtaining a large temporal dynamic range in a FLIM system by using a low repetition rate (10^1 Hz), high output, nitrogen pumped dye laser and a wide-field, intensified CCD camera for image detection. We explore the feasibility of the approach by imaging the oxygen-sensitive dye tris(2,2′-bipyridyl)dichloro-ruthenium(II) hexahydrate (RTDP) in solution and in living cells. We demonstrate the ability of the system to resolve 60% variations in RTDP fluorescence lifetime upon oxygen cycling in solution. Furthermore, the FLIM system was able to resolve an increase in RTDP fluorescence lifetime in cultured human epithelial cells under diminished oxygen conditions. The technique may be useful in developing methods for quantifying intracellular oxygen concentrations.

1. Introduction

Steady-state methods of fluorescence intensity microscopy are routinely employed for studies in cell biology to reveal information regarding cellular morphology, intracellular ion concentrations, protein binding, lipid content, and membrane status [1]. Fluorophore electronic excited-state lifetimes, which depend on both radiative and non-radiative decay mechanisms, offer an additional source of contrast in imaging applications, because they are known to be highly sensitive to local physical conditions in the fluorophore's microenvironment (temperature, *p*H, oxygen concentration, polarity, binding to macromolecules, ion concentration, relaxation through quenching and resonant energy transfer), while being generally independent of factors influencing fluorescence intensity (fluorophore concentration, photobleaching, artefacts arising from optical loss) [2, 3].

Fluorescence lifetime imaging microscopy (FLIM) is relatively a new technique. First reported in 1989 [4], FLIM was subsequently applied to study endosome fusion in single cells [5]. Later, FLIM using the fluorescent probe c.SNAFL-1 was reported for quantitative *p*H determination in living cells and found to compare favourably with the traditional ratiometric technique [6]. The study found that both methods provided accurate information regarding intracellular *p*H, while the lifetime method was easier to employ because no lengthy system calibration was required. FLIM was subsequently applied to phthalocyanine photosensitizer distribution measurement in V79-4 Chinese hamster lung fibroblast cells [7]. The detailed lifetime map obtained was used to distinguish between inhomogeneous distributions of photosensitizers and localized intracellular quenching. The distinction between the two processes could only be made with lifetime imaging and would be impossible with conventional fluorescence intensity microscopy. FLIM experiments using

[1] Author to whom correspondence should be addressed.

a variety of endogenous and exogenous contrast agents have been described in recent reviews [3, 8, 9].

Knowledge of intracellular oxygen levels is important in understanding numerous cellular processes. Of the techniques available for measuring oxygen in cells and tissues (including Clark-type electrodes, fluorescence, electron paramagnetic resonance and nuclear magnetic resonance), only fluorescence based measurements offer the opportunity for non-invasive measurements with the high sensitivity and spatial resolution required for intracellular oxygen sensing [10].

Fluorescence probes based on ruthenium(II) complexes have been used for intracellular oxygen sensing. Such probes rely on fluorescence quenching by oxygen and have been used in both steady-state intensity based measurements [11, 12] (where quenching causes a decrease in fluorescence intensity), as well as lifetime measurements [13–15] (where quenching causes a decrease in fluorophores lifetime). Fluorescence quenching is any physical mechanism resulting in a decrease of fluorescence intensity from a sample [2]. Collisional quenching of fluorescence refers to a process whereby an excited fluorophore molecule is de-excited non-radiatively to its ground state due to physical interactions (collisions) with some agent (quencher). Oxygen is known to be an effective collisional quencher of nearly all known fluorophores. Collisional quenching reduces fluorophore quantum yield (the ratio of emitted fluorescence photons to absorbed excitation photons), resulting in a decrease in emitted fluorescence intensity, as well as a reduction in fluorophore excited-state lifetime. Because steady-state fluorescence intensity measurements will detect decreased fluorescence intensities from a variety of quenching mechanisms (e.g. static quenching or losses due to scattering), decreases in fluorescence lifetimes (which are insensitive to other forms of quenching) are considered to provide distinct proof of collisional quenching in a sample [2]. As indicated above, one advantage of intensity-independent fluorescence lifetime methods is the insensitivity to fluorophore concentration, thereby minimizing artefacts if oxygen-sensitive probes are heterogeneously distributed within the biological sample [12].

Two main methods for FLIM have been explored for biological applications: frequency-domain (FD) and time-domain (TD). FD techniques for measuring lifetimes use amplitude modulated excitation light and detect the shift in phase and amplitude demodulation of the fluorescence signal, whereas TD methods employ pulsed excitation light and detect the resulting fluorescence decay over time [2]. Intracellular fluorescence lifetime imaging of ruthenium-based dyes have been reported using both FLIM implementations. A TD FLIM study by Gerritsen *et al* [13] used an electro-optically chopped argon laser with a repetition frequency of 25 MHz and a confocal scanning microscope to image the oxygen-sensitive dye tris(2,2′-bipyridyl)dichloro-ruthenium(II) hexahydrate (RTDP) in J774 macrophages. The fluorescence lifetime of RTDP in buffer solution was calibrated as a function of oxygen concentration and was in excellent agreement with a Stern–Volmer relation. The lifetime, which ranged from 775 to 425 ns between 0 and 300 μM O_2 in solution, was not sensitive to environmental factors such as pH and ion concentration. In cells, RTDP was found to partition heterogeneously, leading to a nonuniform fluorescence intensity, however a uniform lifetime throughout the cell suggested the oxygen concentration was constant. A FD FLIM study by Malak *et al* [14] also reported successful intracellular imaging of ruthenium-based dyes. Here, the source was modulated at 400 kHz, and similar oxygen-depleted changes in the phase angle were seen inside and outside the macrophage cell. Phototoxicity of ruthenium dyes were investigated by Dobrucki [10], who identified conditions under which ruthenium-based dyes could be used to probe oxygen concentrations within living cells without detectable phototoxic effects. Concentrations below 0.2 mM RTDP were found not to cause measurable photodamage.

While ruthenium-based oxygen sensing shows promise, one difficulty may be in developing FLIM systems that have temporal dynamic ranges large enough to image long fluorescence lifetime dyes. Because most biological fluorophores have lifetimes in the 10^{-9}–10^{-8} s range, as compared with 10^{-6} s for ruthenium-based dyes, FD FLIM systems often use an excitation source modulated in the 10^{7}–10^{8} Hz range to optimize the detection sensitivity of the system to nanosecond lifetime fluorophores. However, FD FLIM systems may be limited in temporal dynamic range [16]. TD FLIM systems have a greater dynamic range, though the increasingly common use of mode-locked Ti : Sapphire lasers makes long lifetime measurements difficult without the use of cavity dumpers or pulse pickers to lower the repetition rate. Therefore, high repetition rate systems may not be optimized for sensing both nanosecond lifetime fluorophores and microsecond lifetime ruthenium-based dyes.

Here, we present an experimental approach for imaging long lifetime fluorophores using a TD FLIM system and demonstrate the feasibility of such a system for oxygen sensing by imaging living cells stained with RTDP. The system used a pulsed, nitrogen-pumped dye laser (tunable from the near UV to NIR wavelengths) and a time-gated, intensified CCD camera. Fast data collection and analysis times (∼20 s) of fluorescence lifetime images were possible despite the low repetition rate of the laser (3 Hz in this study) due to the high per pulse energy of the laser and the wide-field mode of image acquisition. The ability of the system to image nanosecond lifetimes at similar laser repetition rates was shown previously [17]. Thus this study presents a novel approach for simultaneously obtaining large temporal dynamic range and spectral tunability in a TD FLIM system.

We begin in section 2 with a description of the instrument, sample preparation, data acquisition and data analysis methods employed. Section 3 shows the results of our study, including the detection of RTDP lifetime odulation under air-saturated and oxygen diminished conditions, while section 4 discusses the implications of those results to oxygen sensing.

2. Instrumentation and methods

2.1. Fluorescence lifetime imaging microscope

A tunable, wide-field microscopy system was used to obtain two-dimensional fluorescence lifetime images of biological samples with sub-nanosecond resolution. A schematic of the FLIM system is shown in figure 1. The excitation source was a pulsed nitrogen laser (GL-3300, Photon Technology

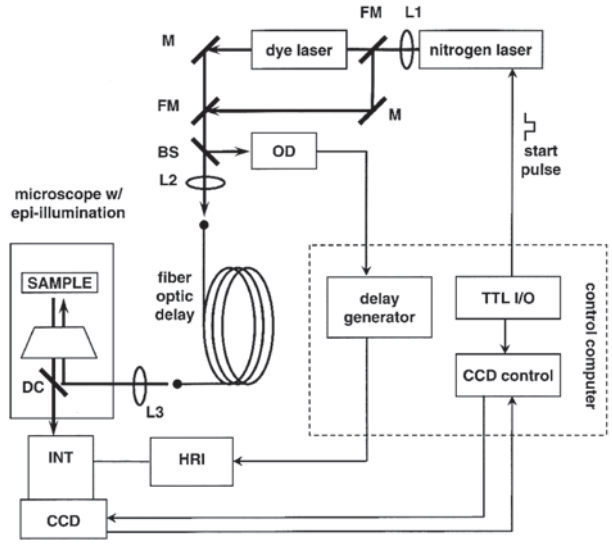

Figure 1. FLIM schematic. Abbreviations: CCD—charge coupled device; HRI—high rate imager; INT—intensifier; TTL I/O—TTL input/output card; OD—optical discriminator. Abbreviations for optical components: BS—beam splitter; DC—dichroic mirror; FM—mirror on retractable 'flip' mount; L1, L2, L3—quartz lenses; M—mirror. Thick solid lines—light path; thin solid line—electronic path.

International, Lawrenceville, NJ) emitting at 337.1 nm. The laser was capable of operating between 1 and 50 Hz and had an output energy of 1.45 mJ per pulse with a pulse width of 0.8 ns. The output of the nitrogen laser could be used either for sample excitation or to pump a tunable, pulsed dye laser (GL-301, Photon Technology International) operating between 365–960 nm. In order to match the excitation spectrum of RTDP, the dye laser operating at 460 nm, with an output energy of 157 μJ per pulse and a pulse width of 0.4 ns, was employed for the experiments described here.

The excitation light was coupled to a 20 m long, 600 μm diameter, 0.22 NA optical fibre (SFS600/660N, Fiberguide Industries, Stirling, NJ) and delivered to a research grade, inverted microscope (Axiovert S100 2TV with lateral and base TV camera ports, Zeiss, Jena, Germany) in epi-illumination mode. The excitation light exiting the fibre was collimated using a quartz lens ($f = 70$ mm) and entered the microscope via the back port of the microscope designed for a commercial UV lamp source. A dichroic mirror (Q495lp, Chroma Technology Corp., Brattleboro, VT) in combination with a long-pass filter (HQ500lp, Chroma Technology Corp.) delivered the beam into a UV compatible Fluar (40×, 1.3 NA, Zeiss) objective for sample excitation. The entrance port was overfilled, and the objective field of view was centred on the peak of the beam profile. An iris before the dichroic was used to control the size of illumination area, providing a uniform illumination with a typical diameter of 150 μm. Energies at the sample were up to 20 μJ/pulse at 460 nm excitation. Due to the low coherence of the source, no speckle was observed.

Artefacts due to temporal jitter in the laser discharge were minimized by using a reference beam split from the main laser itself as the timing reference. An electronic pulse with high temporal stability with respect to the reference beam was generated by means of a constant fraction optical discriminator (OD) (OCF-400, Becker & Hickl GmbH, Berlin, Germany). Output from the OD was sent to a picosecond delay generator (DEL450, Becker & Hickl GmbH), which provided an adjustable time delay with 12-bit delay resolution. The delay generator output was used to trigger the gated, intensified CCD camera.

After sample excitation, the fluorescence emission was collected through the microscope objective and sent to the lateral TV port of the microscope. An ultrafast gated, intensified charge-couple device (ICCD) camera (Picostar HR, La Vision, Goettingen, Germany) was used for image detection. Gate widths were controlled by slaving the ICCD gate to an external logic signal for gate widths adjustable from 10^{-9} to 10^{-3} s. A voltage across the micro-channel plate (MCP), adjustable from 260 to 800 V, provided an adjustable intensifier gain. The MCP voltage was set at 760 V for the RTDP solution and 800 V for cell samples. The output of the intensifier was coupled to a 640 × 480 pixel, 12-bit CCD camera, cooled to −15°C to minimize thermal dark current.

Thus, the system executed the following sequence per each fluorescence image acquisition: the control computer TTL I/O card sent a trigger signal to fire the laser and start the CCD camera exposure; the laser output was split into an excitation and reference pulse (BS, figure 1); the reference pulse initiated the user controlled electronic delay via the OD, while the excitation pulse was delayed through a fibre optic; the excitation pulse entered the microscope and excited the sample, with the ICCD capturing the resulting fluorescence image at the controlled delay time after excitation. After completion of this sequence, the CCD was read off and the image was sent to the computer for analysis and storage.

2.2. Data analysis

Lifetime maps were calculated on a pixel-by-pixel basis by fitting the lifetime of pixel p to the logarithm of the intensity,

$$\ln I_{i,p} = -\frac{t_i}{\tau_p} + C, \tag{1}$$

where $I_{i,p}$ is the intensity of pixel p in image i, t_i is the time delay of image i, and C is a constant. Analytic least squares lifetime fits were:

$$\tau_p = -\frac{N(\sum t_i^2) - (\sum t_i)^2}{N \sum t_i \ln I_{i,p} - (\sum t_i)(\sum \ln I_{i,p})}, \tag{2}$$

where N is the number of images. All sums are over i.

Figure 2 shows the FLIM system response with dye laser excitation ($\lambda_{ex} = 460$ nm), as determined by imaging rose bengal in deionized water for a range of gate delays. Rose bengal was used because its excited-state lifetime was 0.09 ns [18], which is shorter than both the lower limit of the ICCD gate width (0.2 ns, as specified by the manufacturer) and the dye laser pulse duration (0.4 ns). Intensities plotted are the average within a region of interest. The response was fitted to a Gaussian for a FWHM of 0.9 ns. Hence, the FLIM system response was negligible compared with typical lifetimes of the RTDP dye (∼400–800 ns).

Since the lifetime of RTDP is long relative to the system response, the fluorescence emission can be acquired at multiple

gate delays between 200 and 1200 ns to ensure the coverage of two decades of lifetime in calculating the lifetime map. Figure 3 is a schematic illustrating collection of fluorescence from RTDP solution at delays of 400, 600, 800, 1000 and 1200 ns, with the gate width set to 50 ns. Fluorescence from RTDP-loaded cell samples was collected at delays of 200, 400, 600 and 800 ns, with the gate width set to 100 ns. The laser was operated at about 3 Hz for this study, and calculations for creating a 640×480 pixel lifetime image using 5 gates required 15 s using a PC with an AMD K6-2 processor at 300 MHz, for total acquisition and analysis times for lifetime images of about 20 s. Accurate average lifetimes were obtained by creating a histogram based on the lifetime map, fitting it to log-normal functions and calculating the average time from the regression.

2.3. Sample preparation and methods

0.0195 g of RTDP obtained from Aldrich Chemical Co. was diluted in 4 ml of phosphate-buffered saline (PBS) and used as the stock solution at the concentration of 6.5 mM. About 10 μl of the RTDP stock solution was further diluted in 1 ml of PBS

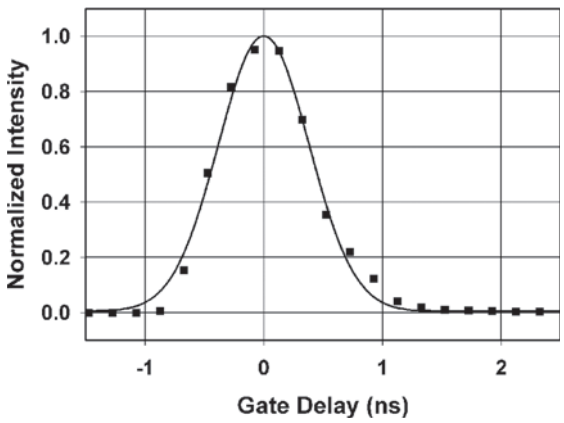

Figure 2. FLIM system response for dye laser excitation of rose bengal in de-ionized water. With 200 ps ICCD gate width, the FWHM is ∼900 ps, showing that the FLIM temporal resolution at 460 nm excitation is ample for measuring the lifetime of RTDP.

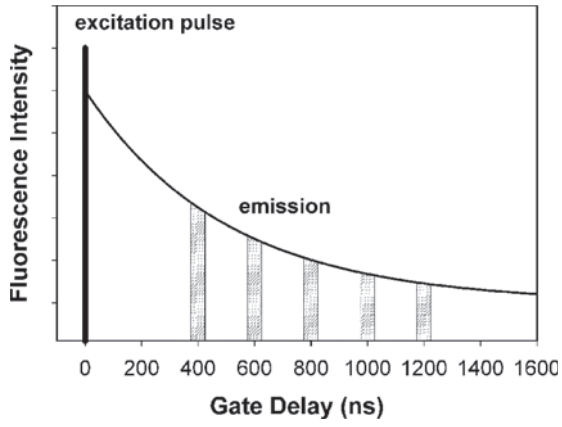

Figure 3. Collecting fluorescence signal at difference gate delays to construct lifetime maps. Fluorescence from the RTDP solution was collected at delays of 400, 600, 800, 1000 and 1200 ns, with a gate width of 50 ns. Fluorescence from RTDP-loaded cell samples was collected at delays of 200, 400, 600 and 800 ns, with a gate width of 100 ns.

(the final concentration of RTDP: 0.064 mM) and transferred to a glass bottomed microwell dish (P35G-0-14-C, MatTeK Corp., Ashland, Massachusetts). A perfusion chamber gasket (C-18136, CoverWell™, Molecular Probes, Eugene, Oregon) was then put on the top of the well at the centre of the dish to form a seal. Oxygen concentration in the RTDP solution was diminished by flowing nitrogen through the holes on opposite ends of the perfusion chamber gasket.

The human bronchial epithelial cell lines (BEAS-2B and BEAS-2B$_{NNK}$) were previously described [19]. BEAS-2B was derived from normal human bronchial epithelial cells and then immortalized via transduction of the SV40 T antigen. BEAS-2B$_{NNK}$ was derived through tobacco-carcinogen-induced transformation of BEAS-2B cells following treatment with *N*-nitrosamine-4-(methylnitrosamino)-1-(3-pyridyl)-1-butanone (NNK). These cell lines provide valuable models for studies seeking to distinguish between normal and malignant cells.

Nonconfluent monolayers of cells were plated on glass bottom microwell dishes and grown in 2 ml of growth medium (LHC-9, Biofluids, Rochville, MD) at 37°C and 5% CO_2 for 2 days until they became 70–75% confluent. Cells were then stained with 50 μl of RTDP stock solution and incubated with RTDP at a final concentration of 0.3 mM for 4–6 h prior to imaging. The cells were washed with PBS at least three times before ∼1 ml of PBS or medium was added. The imaging experiment was carried out at room temperature. Nitrogen gas was bubbled into uncovered cell samples to change the oxygen level.

3. Results

3.1. Lifetime response of RTDP solution upon oxygen cycling

Figure 4 shows a typical cycle of RTDP lifetime upon change of oxygen concentration as obtained from FLIM measurements. The average lifetime of RTDP as determined from the histogram of lifetimes increased from ∼381 to ∼610 ns after flowing nitrogen gas for 18 min. After the solution reached equilibrium, nitrogen flow was stopped and the lifetime of RTDP decreased to ∼384 ns due to quenching by oxygen in about 30 min. The system was cycled more than once and good reproducibility was found for the lifetime

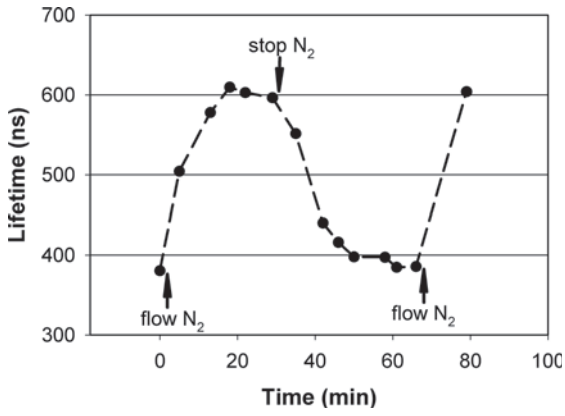

Figure 4. RTDP lifetime can be cycled by diminishing the oxygen level in solution, as measured by the FLIM system.

of RTDP at the equilibrium points. We note that by the end of the experiment, a noticeable amount of PBS had evaporated from the sample due to nitrogen flow, thereby resulting in an increase in the concentration of RTDP solution. This increase in fluorophore concentration was detected as an overall increase in fluorescence intensity, while FLIM maps remained unaffected by concentration changes, thereby illustrating the intensity-independence of fluorescence lifetime imaging. To double check FLIM data analysis, the natural logarithm of the fluorescence intensity was plotted against delay time and checked for linearity to make sure our choices of gate delays and gate width were appropriate.

3.2. Lifetime map of epithelial cells stained with RTDP

Fluorescence images from RTDP-loaded epithelial cell samples were collected with the FLIM system. To improve signal-to-noise, five images were averaged for each gate delay. Because the fluorescence emission was relatively weak, the MCP voltage was set at the highest setting of 800 V for image acquisition. Typical signal strengths at the 200 ns gate were 60–100 camera counts, with a background of 9 counts. The background count for each gate delay, measured in a region of the image without cells, was subtracted from the intensity image before calculation of the lifetime image. The signal could be collected at a gate delay of 200 ns without risk of saturating the ICCD, which had prevented us from using this gate delay when collecting fluorescence from the RTDP solution. Furthermore, the gate delay of 1000 and 1200 ns were not employed since the signal level had dropped significantly and become comparable with noise at these gates. The gate width was chosen to be 100 ns to increase the signal, and we verified that increasing the gate width from 50 to 100 ns did not cause a change of measured RTDP lifetime.

The major source of endogenous cellular fluorescence near the excitation wavelength used here was consistent with fluorescence emission from oxidized flavins [19]. Flavins have excited-state lifetimes in the nanosecond regime [2], two orders of magnitude shorter than that of RTDP. Therefore, endogenous cellular fluorescence was considered negligible at the gate delays used for this study.

FLIM images were taken under air-saturated and oxygen-diminished conditions. Since RTDP was used at a relatively low concentration in the cell sample, no photodamage was observed throughout the experiment, consistent with previous studies [10]. Figure 5 shows a set of representative images taken from BEAS-2B$_{NNK}$ cells. Figure 5(*a*) is a differential interference contrast (DIC) image of 8 cells. Figure 5(*b*) shows the fluorescence intensity image of the same cells before flowing nitrogen. Figures 5(*c*) and (*d*) are the fluorescence lifetime maps of the cells before and after flowing nitrogen for 10 min, showing the increase in lifetime with the decreased oxygen. The lifetime scale on the right has units of nanoseconds.

The natural logarithms of the fluorescence intensity within cells were checked to be linear with the gate delay time, as shown by figure 6(*a*), indicating that our choice of the gate delays and the gate width were proper for measuring the lifetime of RTDP in cell samples via FLIM. Note that the decrease in the slope of the fitted line from air-saturated

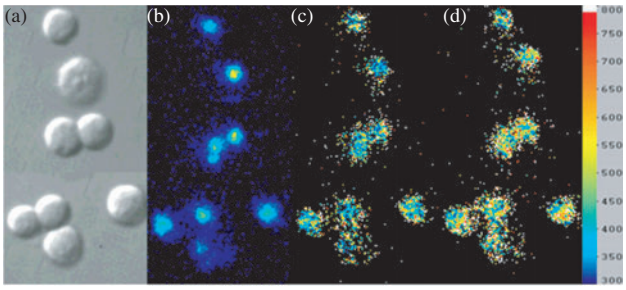

Figure 5. Representative images of BEAS-2B$_{NNK}$ cells taken with FLIM. (*a*) Differential interference contrast image, (*b*) fluorescence intensity image of cells before flowing nitrogen, (*c*) fluorescence lifetime map before flowing nitrogen, (*d*) fluorescence lifetime map after flowing nitrogen for 10 min. The lifetime scale on the right is in nanoseconds.

(circle, I) to oxygen-diminished (square, II) condition suggests an increase in the lifetime. Figure 6(*b*) consists of curves I and II, which were fitted to the histograms of lifetimes from the upper four cells in figures 5(*c*) and (*d*), with FWHM of 242 and 329 ns, respectively. The average lifetime of RTDP fluorescence increased from 421 ns (Curve I) to 521 ns (Curve II), indicating that the lifetime of RTDP increased in the cell samples as a result of decreased oxygen level due to nitrogen flow. The same trend was found with the lower four cells in figure 5, with the lifetime ranging from 441 ns through 526 ns within 10 min, as well as with cells in two other independent FLIM measurements.

4. Discussion

Due to the importance of oxygen in numerous cellular processes, much effort has been spent on developing analytical methods to measure intracellular oxygen levels. Most methods assess intracellular oxygen levels by measuring extracellular oxygen concentration, under the assumption that oxygen levels remain the same throughout the cells, which may not always be valid [12]. Furthermore, the accuracy of oxygen consumption measurements, when applied to groups or suspensions of cells, is limited by factors such as cell counting accuracy. In addition, there are inherent uncertainties associated with some oxygen sensing methods, such as Clark-type electrodes, which consume oxygen during the measurement. RTDP, on the other hand, has been demonstrated to yield a strong luminescent signal in viable cells without causing evident phototoxic effects or measurable photodamage to plasma membranes at a concentration of 0.2 mM [10]. (The concentration of RTDP in our cell samples, ∼0.3 mM, was slightly higher than 0.2 mM. Nevertheless, detectable loss of membrane integrity was found previously only when the extracellular concentration of RTDP reached 1 mM [10].) Unlike other methods for oxygen sensing, such as Clark-type electrodes, which sense extracellular oxygen level or may perturb intracellular oxygen concentrations, FLIM imaging of long excited-state lifetime, ruthenium-based dyes, of which RTDP is one example, holds the promise of non-invasively sensing the oxygen level inside of individual living cells.

Figure 4 shows that the kinetic response of the lifetime of RTDP in solution was reversible, though we noted that a conspicuous amount of PBS had evaporated from the sample

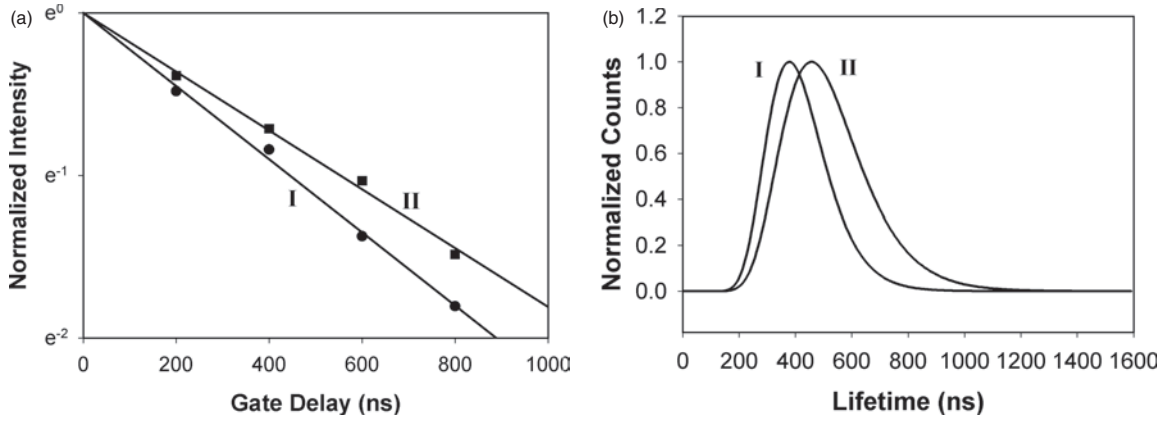

Figure 6. (*a*) Temporal response of RTDP in cell samples under air-saturated (circle, I) and oxygen-diminished (square, II) conditions, as measured by the FLIM system. (*b*) Curves I and II, fitted to the histograms of the upper four cells in figures 5(*c*) and (*d*), respectively. Curve II shifted to the right of Curve I, indicating that the average lifetime of RTDP in the cell samples increased by ∼100 ns as nitrogen flowed over the cells and the oxygen level decreased.

at the end of the experiment due to nitrogen flow, and consequently the detected fluorescence intensity had increased. The insensitivity of the RTDP lifetime to its concentration, as illustrated in figure 4, proved to be useful for its application in cells since the concentration of RTDP within cells varied with cell contents even if the oxygen concentration remained constant, as noted previously [10].

The cells in the DIC image (figure 5(*a*)) colocalized with the RTDP signal in the intensity image (figure 5(*b*)), indicating that the RTDP fluorescence originated from the cells. Since extracellular RTDP was washed away prior to imaging, we conclude that we were imaging intracellular RTDP. However, RTDP did not distribute uniformly within the cells, as shown by figure 5(*b*). In previous studies, it was postulated that RTDP accumulated in cell nuclei and, to a lesser extent, in the cytoplasm after it permeated the cell membrane [10]. This heterogeneous distribution would introduce artefacts if the oxygen level was assessed based on RTDP fluorescence intensity, which is sensitive to both the concentration of RTDP and oxygen. In contrast, the lifetime imaging method based on FLIM was found to be insensitive to RTDP concentration, as noted above.

The modulation of RTDP excited-state lifetime in cells was detected when nitrogen was bubbled into the air-saturated solution containing RTDP-loaded cells. Figure 6 shows the increase of intracellular RTDP lifetime by ∼100 ns as oxygen became depleted by the overflow of nitrogen into the cell sample. Nevertheless, there was some variability in lifetime change between cells, as evidenced by the lifetime change of the upper vs lower four cells in figure 5: 24% vs 19%, respectively. It is unclear to us whether this should be attributed to varying oxygen levels in different cells or factors associated with the sensitivity of RTDP to other cell contents. Future experiments calibrating cellular oxygen concentration in a well-sealed chamber, as well as possibly the oxygen consumption rate, may help to answer this question.

The fluorescence lifetime of RTDP was calibrated in phosphate buffer by Gerritsen *et al* [13], and was found to be independent of pH and ion concentration. The fluorescence lifetime followed the Stern–Volmer relation with $\tau_0/\tau = 0.998+0.002\,73\,[O_2]$, where $[O_2]$ was the concentration in μM, and τ_0 was the lifetime (775 ns) at zero oxygen concentration. Using their calibration, figure 4 represents cycling between oxygen concentrations of 380 and 100 μM, and figure 6 shows a decrease in oxygen concentration from 310 to 180 μM. Future experiments in a well-sealed chamber are needed verify lifetime calibration.

Histograms of different cell clusters were created based on their lifetime maps (figure 6(*b*)). One factor increasing the width of the histogram was the intensification of noise due to the large intensifier MCP voltage (800 V) needed for the cellular measurements. Noise broadened the histogram because lifetimes were calculated on pixel-by-pixel basis. Signal averaging, such as image smoothing, narrows the lifetime histogram, possibly improving lifetime resolution, but at the expense of spatial resolution. Both factors must be considered when determining the resolution of this technique.

Fast acquisition and analysis times (∼20 s) were achievable because the high per pulse energy (microjoules) of the laser and the wide-field image acquisition by the ICCD permitted the entire fluorescence image at a given gate delay to be captured with reasonable signal-to-noise using only a few laser shots. This is in comparison to FLIM methods using high repetition rate lasers, such as Ti : Sapphire lasers, which have lower per pulse energies (nano- to picojoules), but integrate over a significantly larger number of pulses resulting in comparable acquisition times [20].

Because the FLIM system presented here is also tunable down to 337.1 nm excitation, near simultaneous sensing of intracellular oxygen and endogenous fluorophores related to cellular respiration would be possible. Since endogenous fluorophores, including reduced pyridine nucleotides and oxidized flavins, are involved in aerobic pathways, monitoring their fluorescence has provided a useful tool for assessing cellular metabolic activity [21]. Several design features of the FLIM system make it useful for studies combining oxygen sensing and metabolic imaging. The nitrogen-pumped dye laser provides a high flux, tunable pulsed excitation source. The fast-gated ICCD is capable of single-photon detection, with gate widths as short as 200 ps. Rapid adjustment of excitation wavelength is possible by means of retractable mirrors (FM; figure 1), and there is low jitter in temporal

gating regardless of excitation wavelength because timing is synchronized with an OD using a pulse split from the main pulse just prior to entering the optical delay fibre. The ability to extract excited-state lifetimes in the sub-nanosecond regime with near-UV excitation has been demonstrated for this system [17].

The preliminary results presented here demonstrate the FLIM imaging of a ruthenium-based dye potentially useful in sensing intracellular oxygen concentrations in living cells. Unlike steady-state fluorescence intensity measurements, which can be affected by non-uniform distribution of RTDP within cells [10], difference in the uptake of RTDP between cells, and leakage of RTDP out of the cells [13], lifetime-based sensing is less sensitive to RTDP concentration. Because long excited-state lifetimes may be difficult to measure with high repetition rate FLIM systems, we present an experimental approach using a high flux, low repetition rate laser to obtain a large temporal dynamic range. Previously, the system was shown to have spectral tunability to near-UV excitation wavelengths with accurate recovery of excited-state lifetimes in the sub-nanosecond regime [17]. To conclude, FLIM holds the potential of being developed into a fast, non-invasive system for intracellular oxygen sensing using ruthenium-based dyes, which could provide useful information on important biological activities in living systems.

Acknowledgments

The authors would like to thank Professors E Dmitrovsky and K H Dragnev for providing us with access to the human bronchial epithelial cell lines. This work was supported by The Whitaker Foundation (M-AM).

References

[1] Rudolph W and Kempe M 1997 Topical review: trends in optical biomedical imaging *J. Modern Opt.* **44** 1617–42

[2] Lakowicz J R 1999 *Principles of Fluorescence Spectroscopy* 2nd edn (New York: Kluwer Academic/Plenum)

[3] Tadrous P J 2000 Methods for imaging the structure and function of living tissues and cells: 2. Fluorescence lifetime imaging *J. Pathol.* **191** 229–34

[4] Bugiel I, König K and Wabnitz H 1989 Investigation of cell by fluorescence laser scanning microscopy with subnanosecond time resolution *Lasers Life Sci.* **3** 47–53

[5] Oida T, Sako Y and Kusumi A 1993 Fluorescence lifetime imaging microscopy (filmscopy): methodology development and application to studies of endosome fusion in single cells *Biophys. J.* **64** 676–85

[6] Sanders R, Draaijer A, Gerritsen H C, Houpt P M and Levine Y K 1995 Quantitative pH imaging in cells using confocal fluorescence lifetime imaging microscopy *Anal. Biochem.* **227** 302–08

[7] Scully A D, MacRobert A J, Botchway S, O'Neill P, Parker A W, Ostler R B and Phillips D 1996 Development of a laser-based fluorescence microscope with subnanosecond time resolution *J. Fluorescence* **6** 119–25

[8] Gadella T W J Jr 1999 Fluorescence lifetime imaging microscopy (FLIM): instrumentation and application, ed W T Masons *Fluorescent and Luminescent Probes for Biological Activity* (San Diego: Academic) 467–79

[9] Urayama P and Mycek M-A (ed) 2003 Fluorescence lifetime imaging microscopy of endogenous biological fluorescence *Handbook of Biomedical Fluorescence* ed M-A Mycek and B W Pogue (New York: Marcel-Dekker Inc.) 211–36

[10] Dobrucki J W 2001 Interaction of oxygen-sensitive luminescent probes $Ru(phen)_3^{2+}$ and $Ru(bipy)_3^{2+}$ with animal and plant cells in vitro: mechanism of phototoxicity and conditions for non-invasive oxygen measurements *J. Photochem. Photobiol. B: Biol.* **65** 136–44

[11] Asiedu J K, Ji J, Nguyen M, Rosenzweig N and Rosenzweig Z 2001 Development of a digital fluorescence sensing technique to monitor the response of macrophages to external hypoxia *J. Biomed. Opt.* **6** 116–21

[12] Ji J, Rosenzweig N, Jones I and Rosenzweig Z 2002 Novel fluorescent oxygen indicator for intracellular oxygen measurements *J. Biomed. Opt.* **7** 404–09

[13] Gerritsen H C, Sanders R, Draaijer A and Levine Y K 1997 Fluorescence lifetime imaging of oxygen in living cells *J. Fluorescence* **7** 11–16

[14] Malak H, Dobrucki J W, Malak M M and Swartz H M 1998 Oxygen sensing in a single cell with ruthenium complexes and fluorescence time-resolve microscopy *Biophys. J.* **74** A189

[15] Castellano F N and Lakowicz J R 1998 A water-soluble luminescence oxygen sensor *Photochem. Photobiol.* **67** 179–83

[16] Philip J and Carlsson K 2003 Theoretical investigation of the signal-to-noise ratio in fluorescence lifetime imaging *J. Opt. Soc. Am.* A **20** 368–79

[17] Urayama P, Zhong W, Beamish J A, Minn F K, Sloboda R D, Dragnev K H, Dmitrovsky E and Mycek M-A 2003 A UV-visible fluorescence lifetime imaging microscope for laser-based biological sensing with picosecond resolution *Appl. Phys. B: Lasers Opt.* at press

[18] Ware W R, Pratinidhi M and Bauer R 1983 Performance characteristics of a small side-window photomultiplier in laser single-photon fluorescence decay measurements *Rev Sci. Instrum.* **54** 1148–56

[19] Pitts J, Sloboda R, Dragnev K, Dmitrovsky E and Mycek M-A 2001 Autofluorescence characteristics of immortalized and carcinogen-transformed human bronchial epithelial cells *J. Biomedical Opt.* **6** 31–40

[20] Webb S E D *et al* 2002 A wide-field time-domain fluorescence lifetime imaging microscope with optical sectioning *Rev. Sci. Instrum.* **73** 1898–907

[21] Chance B, Schoener B, Oshino R, Itshak F and Nakase Y 1979 Oxidation-reduction ratio studies of mitochondria in freeze-trapped samples *J. Biol. Chem.* **254** 4764–71